

Dear Mr. Brown,

Thank you for your comments on the manuscript and we have finished the revision based on your comments. Also, all authors have proofread the manuscript several times to make sure that the paper is free of grammatical and technical errors, as well as to make sure the content is properly presented. Thanks again for your work on handling our manuscript.

Zeshi Zheng

Major comment,

I suggest you include the answers to your three questions in the abstract and conclusions. Note that as posed, your Question 2 is difficult to understand.

1. What new information about orographic effects on precipitation versus accumulation is provided by Lidar data?
2. Is it possible to have snow-depth measurements in forested mountain terrain from all pixels on a fine sampling resolution (1- to 5 m) using Lidar data? If not, how does the percentage of pixels measured change with the sampling resolution. [Not clear what you mean by a "measured" pixel]
3. Third, what is the importance of slope, aspect and canopy penetration fraction on snow accumulation, relative to elevation; and are effects consistent across sites?

Response: Both abstract and conclusions have been revised and now include quantitative results. Question 2 was re-phrased and now it should be easier to understand.

Minor comment,

Lines 17-18: It seems there is a key word missing in the sentence. "...the percent of pixels with [valid?] snow-depth measurements is..."

Response: The sentence was changed to "...the percent of pixels with at least one ground return is..."

Lines 20-29: The results presented in these lines are not clear and quantitative. I suggest you simplify this to something like "Elevation was the dominant physiographic variable explaining snow depth variability over the study regions (xx % of variability) followed by slope (xx%), aspect (xx%) and canopy penetration fraction (xx%). However, the relative importance of the latter three variables was observed to vary with elevation and canopy-cover."

Response: Quantitative results are included in the abstract. Please see major comment.

Lines 232-234: Not clear. Suggest "A multivariate linear-regression model was also applied to quantify the influence of the various physiographic variables on the snowpack distribution."

Response: Fixed.

line 372: Not clear. Suggest rewording "Based on the scatterplots in shown in Figures 6a and 6b color coded by northness,..."

Response: Fixed.

lines 391-395: This paragraph is confusing and does not provide a clear conclusion. I suggest you cut this.

Response: The paragraph was deleted.

lines 399-401: Suggest you provide some more quantitative estimates of the relative importance of the physiographic variables e.g. were the correlations statistically significant? The conclusions section needs to answer your three questions and indicate what new findings were obtained.

Response: Quantitative results are included in the conclusions. Please see major comment.

I suggest you include an acknowledgement to your reviewers. If it wasn't for Reviewer 2 this paper would never have made it this far!

Response: Acknowledgement to reviewers and editor is included in the manuscript.

Figure 2: Good but could do a better job of conveying the sampling issue e.g. open snow, snow in gaps, and snow under vegetation.

Response: The figure was revised for better presentation.

1 **Topographic and vegetation effects on snow accumulation in**
2 **the southern Sierra Nevada: a statistical summary from Lidar**
3 **data**

4
5 **Z. Zheng¹, P. B. Kirchner^{2,3}, R. C. Bales^{1,4}**

6 [1] Department of Civil and Environmental Engineering, UC Berkeley, Berkeley, CA, USA

7 [2] Joint Institute for Regional Earth System Science and Engineering, Pasadena, CA, USA

8 [3] Southwest Alaska Network, National Park Service, Anchorage, AK, USA

9 [4] Sierra Nevada Research Institute, UC Merced, Merced, CA, USA

10

11 Correspondence to: Z. Zheng (zeshi.z@berkeley.edu)

12 **Abstract**

13 Airborne light detection and ranging (Lidar) measurements in the southern Sierra Nevada near
14 peak snow accumulation in 2010, and in the snow-free season, were analyzed for topographic
15 and vegetation effects on snow accumulation. Point-cloud data were processed from four,
16 primarily mixed-conifer, forest sites separated by 10 to 64 km with a total surveyed area over
17 106 km². It was observed that the percentage of pixels with at least one ground return and thus a
18 snow-depth measurement increases from 65-90% to 99% as the sampling resolution of Lidar
19 point cloud changes from 1 m to 5 m. With about 28% of the area in dense mixed-conifer forest
20 in the main snow-producing elevations of 2000-3000 m having no returns at 1-m resolution,
21 undersampling of snow depth under dense canopies resulted in at least a 10-cm overestimation
22 error in the average snow depth. The 1-m gridded data show consistent patterns over the four
23 sites, dominated by orographic effects on precipitation. Elevation explained 43% of snow-depth
24 variability, with slope, aspect and canopy penetration fraction explaining another 14% over the
25 elevation range of 1500-3300 m. Although, the relative importance of the four variables varied
26 with elevation and canopy cover, all were statistically significant over the area studied. The
27 difference in mean snow depth in open areas versus under canopy increased with elevation in the
28 rain-snow transition zone (1500-1800 m); and was about 35 ± 10 cm above 1800 m, with the 20-
29 cm fluctuation range reflecting the effects of other topographic variables.

30 **1. Introduction**

31 In the western United States, ecosystem processes and water supplies for agricultural and
32 urban users depend on the mountain snowpack as the primary source of late-spring and early
33 summer streamflow (Bales et al., 2006). Knowledge of spring snowpack conditions within a
34 watershed is essential if water availability and flood peaks following the onset of melt are to be
35 accurately predicted (Hopkinson et al., 2001). California's multi-billion dollar agricultural
36 economy as well as multi-trillion dollar urban economy depend on these predictions (California
37 Department of Water Resources, 2013). Both topographic and vegetation factors are important in
38 influencing the snowpack conditions, as they closely interact with meteorological conditions to
39 affect precipitation and snow distribution in the mountains (McMillen, 1988; Raupach, 1991;
40 Wigmosta et al., 1994). However, mountain precipitation is poorly understood at multiple spatial
41 scales because it is governed by processes that are neither well measured nor accurately
42 predicted (Kirchner et al., 2014). Snow accumulation across the mountains is primarily
43 influenced by orographic processes, involving feedbacks between atmospheric circulation and
44 terrain (Roe, 2005; Roe and Baker, 2006). In most forested regions, snow distribution is highly
45 sensitive to vegetation structure (Anderson et al., 1963; Revuelto et al., 2015; Musselman et al.,
46 2008); and canopy interception, sublimation as well as unloading result in less accumulation of
47 snow beneath the forest canopies in comparison with canopy gaps (Berris and Harr, 1987;
48 Golding and Swanson, 1986; Mahat and Tarboton, 2013; Sturm, 1992).

49 The Sierra Nevada serves as a barrier to moisture moving inland from the Pacific, has an
50 ideal orientation for producing orographic precipitation, and thus exerts a strong influence on the
51 upslope amplification of precipitation (Colle, 2004; Rotach and Zardi, 2007; Smith and Barstad,
52 2004). Recent studies provide insight on how orographic and topographic factors affect snow

53 depth in the Alps (Grünewald et al., 2013; Grünewald, et al., 2014; Lehning et al., 2011),
54 suggesting that similar studies could be extended to the Sierra Nevada. And among the forested
55 regions of the mountains, the mixed-conifer and subalpine zones cover most of the high-
56 elevation, seasonally snow-covered area.

57 *In situ*, operational measurements of snow water equivalent (SWE) in the Sierra Nevada
58 come from monthly manual snow surveys and daily snow-pillow observations (Rosenberg et al.,
59 2011). Meteorological stations and remote-sensing products also provide estimates of
60 precipitation and snow accumulation (Guan et al., 2013). Cost, data coverage, accuracy (Julander
61 et al., 1998) and basin-scale representativeness are issues for *in situ* monitoring of SWE in
62 mountainous terrain (Rice and Bales, 2010). Satellite-based remote sensing, such as MODIS, has
63 been used to map snow coverage in large or even global areas. However, it only provides snow-
64 coverage information in open areas, and no direct information on snow depths (Molotch and
65 Margulis, 2008). The SNOW Data Assimilation System (SNODAS) integrates data from satellite
66 and *in situ* measurements with weather-forecast and physically based snow models, providing
67 gridded SWE and snow-depth estimates (Barrett, 2003). However, since SNODAS has not been
68 broadly assessed (Clow et al., 2012), its potential for evaluating snow distribution in mountain
69 areas remains uncertain. Also, owing to its 1-km spatial resolution, the snow depth that
70 SNODAS provides is a mixed representation of both open and canopy-covered areas.

71 An orographic-lift effect is observable in most of the above data (Howat and Tulaczyk,
72 2005; Rice et al., 2011), and a binary-regression-tree model using topographic variables as
73 predictors has also been used for estimating the snow depth in unmeasured areas (Erickson et al.,
74 2005; Erxleben et al., 2002; Molotch et al., 2005). However, regression coefficients could not be
75 estimated accurately for most of the explanatory variables, except for elevation; and the

76 consistency of the orographic trend as well as the relative importance of these variables is still
77 unknown owing to the lack of representative measurements across different slopes, aspects and
78 canopy conditions. Also, the stability of the variance explained by the model needs to be tested
79 with denser measurements.

80 In recent years, airborne Lidar has been used for high-spatial-resolution distance
81 measurements (Hopkinson et al., 2004), and has become an important technique to acquire
82 topographic data with sub-meter resolution and accuracy (Marks and Bates, 2000). Therefore,
83 Lidar provides a potential tool to help understand spatially distributed snow depth across
84 mountain regions. With multiple returns from a single laser pulse, Lidar has also been used to
85 construct vegetation structures as well as observe conditions under the canopy, which helps
86 produce fine-resolution digital elevation models (DEMs), vegetation structures, and snow-depth
87 information. However, the snow depth under canopy can not always be measured because of the
88 signal-intensity attenuation caused by canopy interception (Deems and Painter, 2006; Deems et
89 al., 2006). A recent report applied a univariate-regression model to the snow depth measured in
90 open areas using Lidar; with a high-resolution DEM used to accurately quantify the orographic-
91 lift effect on the snow accumulation just prior to melt (Kirchner et al., 2014). From this analysis
92 it could be expected that Lidar data might also help explain additional sources of snow
93 distribution variability in complex, forested terrain.

94 The objective of the work reported here is to improve our understanding of how
95 topographic and vegetation attributes affect snow accumulation in mixed-conifer forests. Using
96 Lidar data from four headwater areas in the southern Sierra Nevada, we addressed the following
97 three questions. First, in forested mountain terrain what percentage of pixels have ground returns
98 and thus provide snow-depth measurements at 1-m and coarser sampling resolutions, and what

99 potential error is introduced by undersampling of snow under dense canopies? Second, what new
100 information about orographic effects on precipitation versus accumulation is provided by these
101 Lidar data? Third, what is the effect of slope, aspect and canopy penetration fraction on snow
102 accumulation, relative to elevation; and are effects consistent across sites?

103 **2. Methods**

104 **2.1 Study Areas**

105 Our study areas are located in the southern Sierra Nevada, approximately 80 km east of
106 Fresno, California (Figure 1). The four headwater-catchment research areas, Bull Creek,
107 Shorthair Creek, Providence Creek, and Wolverton Basin were previously instrumented,
108 including meteorological measurements, in order to have a better knowledge of the hydrologic
109 processes in this region (Bales et al., 2011; Hunsaker et al., 2012; Kirchner et al., 2014). The
110 sites were chosen as part of multi-disciplinary investigations at the Southern Sierra Critical Zone
111 Observatory, and are also the main instrumented sites in the observatory. Wolverton is
112 approximately 64 km southeast of the other three sites (Figure 1) and is located in Sequoia
113 National Park. Both snow-on and snow-off airborne Lidar were flown in 2010 (Table 1) over
114 these sites. The elevation of the survey areas is from 1600-m to 3500-m elevation. Vegetation
115 density generally decreases in high-elevation subalpine forest, with Wolverton also having a
116 large area above treeline (Goulden et al., 2012). The precipitation has historically been mostly
117 snow in the cold and wet winters for elevations above 2000 m, and a rain-snow mix below 2000
118 m, where most of Providence is located. The comparison between Providence and the other sites
119 can help in assessing if observed trends are consistent above and below the rain-snow transition.

120 **2.2 Data Collection**

121 All airborne Lidar surveys were performed by the National Center for Airborne Laser
122 Mapping (NCALM) using Optech GEMINI Airborne Laser Terrain Mapper. The scan angle and
123 scan frequency were adjusted to ensure a uniform along-track and across-track point spacing
124 (Table 2), with six GPS ground stations used for determining aircraft trajectory. The snow-on
125 survey date was close to April 1st, which is used by operational agencies as the date of peak snow
126 accumulation for the Sierra. Since the snow-on survey required four days to cover the four study
127 areas, time-series *in situ* snow-depth data measured continuously from Judd Communications
128 ultrasonic depth sensors at Providence, Bull and Wolverton were used to estimate changes in
129 snow depth during the survey period. While no snow accumulation was observed, snowpack
130 densification and melting observed from the time-series data were taken into considerations
131 (Hunsaker et al., 2012; Kirchner et al., 2014). The snow-off survey was performed in August
132 after snow had completely melted out in the study areas.

133 **2.3 Data Processing**

134 Raw Lidar datasets were pre-processed by NCALM and are available from the NSF
135 Open-Topography website (<http://opentopography.org>) in LAS format. The LAS point cloud,
136 including both canopy and ground-surface points, are stored and classified as ground return and
137 vegetation return. The 1-m resolution digital-elevation models, generated from the Lidar point-
138 cloud datasets, were downloaded from the OpenTopography database and further processed in
139 ArcMap 10.2 to generate 1-m resolution slope, aspect, and northness raster products. Northness
140 is an index for the potential amount of solar radiation reaching a slope on a scale of -1 to 1,
141 calculated from:

$$142 \quad N = \sin(S) \times \cos(A), \quad (1)$$

143 where N is the northness value; S is the slope angle and A is the aspect angle, both in degrees.
144 For aspect angle A , north is either 0° or 360° . Northness is also the same as the aspect intensity
145 (Kirchner et al., 2014) with 0° focal aspect. Since in this analysis the snow-depth comparison is
146 only discussed between north and south facing slopes, northness is used instead of aspect
147 intensity for simplification. To construct the 1-m resolution canopy-height models from Lidar
148 data, the 1-m digital-elevation models were subtracted from the 1-m digital-surface models that
149 were rasterized from the first return of the laser pulses (Figure 2).

150 The snow depths were calculated directly from the snow-on Lidar data. By referring to
151 canopy-height models, all ground points in snow-on Lidar datasets were classified as under
152 canopy or in open areas. That is, if the ground point was coincident with canopy of >2 -m height,
153 it was classified as under canopy, and otherwise in the open, i.e., a 2-m height was used to
154 classify shrubs versus trees. In this study we assumed that shrubs did not affect the snow depth.
155 After classification, snow depths were calculated by subtracting the values in the digital-
156 elevation model from the snow-on point-measurement values. The calculated point snow-depth
157 data were further assigned into 1-m raster pixels, averaged within each pixel, formatted and then
158 gap filled by interpolation with pixel values around it. Since not all laser pulses that generated
159 canopy-surface returns had ground returns (Figure 3) and the ground-return percentage varied
160 across the transition from the tree trunk to the edge of the canopy, interpolation was not applied
161 to data under the canopy. The error rate of the calculated snow depth should be mainly from the
162 instrumental elevation error, which is about 0.10 m (Kirchner et al., 2014; Nolan et al., 2015).

163 **2.4 Penetration Fraction**

164 The open-canopy fraction is a factor that represents the forest density above a given pixel
165 and is used to describe the influence of vegetation on snow accumulation and melt. However

166 there is no algorithm to directly extract this information from Lidar data. Here we use a novel
167 approach that we call penetration fraction to approximate the open-canopy fraction from the
168 Lidar point cloud. With it we were able to quantify the impact of canopy on snow depth using
169 linear regression. Penetration fraction is the ratio of the number of ground points to number of
170 total points within each pixel (Figure 4a). Whereas pixels are generally classified as under
171 canopy or in the open (Kirchner et al., 2014), penetration fraction is an index of fraction open in
172 a pixel. Because the electromagnetic radiation from both Lidar and sunlight beams are
173 intercepted by canopies, the open-canopy fraction is used here as an index to represent the
174 fraction of sunlight radiance received on the ground under vegetation. Therefore, penetration
175 fraction of Lidar is actually another form of estimating the open-canopy fraction (Musselman et
176 al., 2013). However, under-canopy vegetation can also intercept the Lidar beam, causing a bias.
177 To eliminate this bias, the canopy-height model was used to check if the pixel was canopy
178 covered by using the 2-m threshold value; and if not, the local penetration fraction of the pixel
179 was reset to 1 because the open-canopy fraction of a pixel could not be entirely represented by
180 the penetration fraction. A spatial moving-average process was applied using a 2-D Gaussian
181 filter to account for the effect of the vegetation around each pixel. Since the radius of the
182 Gaussian filter needs to be specified by the user, we tested the sensitivity of smoothing results to
183 the radius of the filter and found it is not sensitive when the radius is greater than 1.5 m (Figure
184 4b). Therefore, we specified a radius of 5 m in the Gaussian filter.

185 **2.5 Statistical Analysis**

186 The 1-m resolution snow-depth raster datasets were resampled into 2-m, 3-m, 4-m and 5-
187 m resolution. The percentage of pixels with snow-depth measurements was calculated by using
188 the number of pixels with at least one ground return divided by the total number of pixels inside

189 each site. The sensitivity of the percentage changes across different resampling resolutions and
190 the consistency of the percentages across study sites at the same resampling resolution were
191 analyzed by visualizing the percentages against sampling resolutions at all sites.

192 Using elevation, slope, aspect, penetration fraction and snow depth retrieved from Lidar
193 measurements, topographic and vegetation effects on snow accumulation were observed using
194 residual analysis. Owing to orographic effects, there is increasing precipitation along an
195 increasing elevation gradient in this area (Kirchner et al., 2014). Therefore, elevation was
196 selected as the primary variable to fit the linear-regression model for calculating the residual of
197 snow depth. All snow-depth measurements from Lidar were first separated by either under
198 canopy or in open areas, and then were binned by elevation of the location where they were
199 measured, with a bin size of 1-m elevation. As each elevation band had hundreds of snow-depth
200 measurements after binning, the average of all snow depths was chosen as the representative
201 snow depth, and the standard deviation calculated to represent the snow-depth variability within
202 each elevation band. Coefficients of determination between snow depth and elevation of each
203 site were calculated by linear regression. The fitted linear-regression model of each site was
204 applied to the DEM to estimate the snow depth. The residual of snow depth was calculated by
205 subtracting the modeled snow depth from Lidar-measured snow depth. The slope, aspect and
206 penetration fraction were binned into 1° slope, 1° aspect, and 1% penetration-fraction bins with
207 snow-depth residuals corresponding to each bin of every physiographic variable averaged and
208 visualized along the variable gradient to check the existence of these physiographic effects.

209 For the variables found to correlate with the snow accumulation, the relative importance
210 of each variable was calculated using the Random Forest algorithm (Breiman, 2001; Pedregosa

211 et al., 2011). A multivariate linear-regression model was also applied to quantify the influence of
212 the various physiographic variables on the snowpack distribution.

213 To calculate the snow-depth difference between open and canopy-covered areas along an
214 elevation gradient, the 1-m resolution snow-depth data of the two conditions, open and canopy
215 covered, were smoothed separately against elevation using locally weighted scatterplot
216 smoothing (LOESS) (Cleveland, 1979). The snow-depth difference was then calculated by
217 subtracting the smoothed canopy-covered snow depth from that in the open.

218 **3. Results**

219 The percentage of pixels having snow-depth measurements is sensitive to the sampling
220 resolution used in processing the Lidar point cloud to produce the raster data. Values go from
221 about 65-90% across the 4 sites for 1-m resolution and gradually increase to 99% at 5-m
222 resolution (Figure 5). Note that the percentage increases in going from the lower- to higher-
223 elevation sites, reflecting lower forest density at higher elevation.

224 The snow depths in open areas and under canopy show consistent increases with
225 elevation across all sites (Figure 6a, 6b). Although orographic effects may vary between
226 individual storms across sites, these data suggest that the cumulative effect of the 4 main
227 snowfall events prior to the Lidar flight (Kirchner, 2013) resulted in similar patterns. The
228 variability within an elevation band for open areas (Figure 6c) is highest at about 1500 m, and
229 gradually decreases within the rain-snow transition up to 2000-m elevation. However, above
230 2000 m the pattern of variability with increasing elevation varies across sites. Note that values at
231 the upper or lower ends of elevation at each site have few pixels and thus may not have a
232 representative distribution of other physiographic attributes (Figure 6d). The forested area of all

233 four sites combined spans the rain-snow transition zone in lower mixed-conifer forest through
234 snow-dominated subalpine forest, with significant areas above treeline higher up.

235 For each individual site, a least-squares linear regression of averaged snow depth versus
236 elevation was used to investigate the spatial variability of snow depth (Table 3). The median
237 elevation of the three sites increases from Providence to Bull to Shorthair. The lowest elevation
238 at Providence Creek is less than 1400 m, and snow depth increases steeply in this region at a rate
239 of 38 cm per 100 m in open areas and 28 cm per 100 m under the canopy. Bull Creek has an
240 elevation range of 2000-2400 meters, which is slightly higher than Providence, and has snow
241 depth increasing at 21 cm per 100 m in open areas and 19 cm per 100 m under the canopy. For
242 Shorthair Creek site, which is the highest of the three, the snow depth increases at 17 cm per 100
243 m in open areas and 16 cm per 100 m under the canopy. Wolverton is 64 km further south and
244 spans a wider elevation range, going from the rain-snow transition in mixed conifer, to subalpine
245 forest, to some area above treeline. The average snow-depth increase is smallest among all four
246 study sites, 15 cm per 100 m in open areas and 13 cm per 100 m under the canopy. Unlike the
247 other three lower-elevation sites, the snow depth at Wolverton decreases above 3300-m elevation
248 and these high-elevation data were not included in the linear regression. The amount of area
249 above this elevation is relatively small, and factors such as wind redistribution and the
250 exhaustion of perceptible water can also affect snow depth at these elevations (Kirchner et al.,
251 2014).

252 The residuals for snow in open areas were further analyzed for effects of slope, aspect
253 and penetration fraction. The snow-depth residuals are negative and larger in magnitude on
254 steeper slopes, i.e. less snow on steeper slopes (Figure 7a). The residual also changes from
255 positive to negative with aspect, reflecting deeper snow on north-facing versus south-facing

256 slopes (Figure 7b). The topographic effect can also be seen from the color pattern of northness
257 observed in the scatterplots (Figure 6a, 6b). The residual also changes from negative 20-40 cm to
258 positive 20-40 cm as penetration fraction increases from 0% to 80%, reflecting less snow under
259 canopy (Figure 7c). Considering all of these variables together, elevation is the most important
260 variable at all sites except for Shorthair, which has a relatively small elevation range (Figure 8).
261 Aspect exerts a stronger influence than do slope and penetration fraction in open areas. However,
262 for under-canopy areas, penetration is more dominant than aspect at two sites. The multivariate
263 regression model was fitted to the data with aspect transformed into 0° to 180° range (north to
264 south). Fitted models can be represented as the following two equations for open area and under
265 canopy respectively:

$$266 \quad SD = 0.0011 \times Elevation - 0.0112 \times Slope - 0.0057 \times Aspect + 0.1802 \times Penetration \quad (2)$$

$$267 \quad SD = 0.0009 \times Elevation - 0.0128 \times Slope - 0.0046 \times Aspect + 0.9891 \times Penetration \quad (3)$$

268 where *SD* is snow depth and p-values of all regression coefficients of the two models are all
269 smaller than 0.01. The effects quantified in these two equations are mixtures of influences that
270 affected both precipitation and post-deposition processes.

271 The snow-depth difference between open and canopy-covered areas was calculated with
272 elevation from locally smoothed snow depth. It generally increases from near zero at 1500 m,
273 where there is little snow but dense canopy, to 40 cm in the range of 1800-2000 m, and varies
274 from near zero to 60 cm at higher elevations where snow is deeper and the canopy less dense
275 (Figure 9). It is apparent that the snow-depth difference increases with elevation in the rain-snow
276 transition zone, but lacks a clean pattern along either elevation gradient or penetration-fraction
277 gradient when the elevation is higher.

278 **4. Discussion**

279 **4.1 Sensitivity of measurements to sampling resolution**

280 The results of analyzing the percentage of pixels with snow depth measured by Lidar at
281 different sampling resolutions illustrate that even high-density airborne Lidar measurements do
282 not have 100% coverage of the surveyed area at 1-m resolution, especially in densely forested
283 areas. According to the snow-depth difference between snowpack in open areas and under
284 canopy, a trade-off between accuracy and coverage happens when adjusting the resolution; and
285 lower sampling resolutions can introduce overestimation into the results. This is because upon
286 averaging, sub-pixel area under the canopy that was not measured may be represented by the
287 open area that is measured, introducing an overestimation error into the averaged snow depth of
288 the pixel. In order to estimate that bias for each pixel, we would need more under-canopy snow-
289 depth measurements at 1-m resolution. In our survey areas, 28% of the total area in the main
290 snow-producing elevations of 2000-3000 m has no returns at 1-m resolution. Assuming that
291 using open rather than under-canopy values would introduce a bias of at least 35 cm for these
292 unmeasured areas, a 2-m mean snow depth will have about 10 cm or 5% overestimation over the
293 whole area. The overestimation could be higher if the area with no returns represents denser
294 canopy with less snow than the under-canopy areas measured; and could also be more significant
295 for shallower snowpacks. It would also be higher for a less-dense point cloud, which would
296 introduce uncertainty into both percentage canopy cover and open versus under-canopy snow-
297 depth differences. Therefore, the sampling resolution for processing the Lidar point cloud needs
298 to be chosen according to the objective and accuracy tolerance of the study and the average
299 overestimation bias needs to be corrected for the study results.

300 **4.2 Physiographic effects on snow accumulation**

301 Below 3300 m, the increasing trend of snow accumulation with elevation was observed
302 for all sites (Figure 6). Linear regression is applicable to model the relationship between snow
303 depth and elevation when the study area has a broad elevation range. This holds true for all of
304 our sites with the exception of Shorthair, where the elevation range is about 200 m and the
305 coefficient of determination for this linear-regression model is much smaller than for the other
306 three sites, which have ranges greater than 500 m. The bias of mean snow depth in the same
307 elevation band between different sites is acceptable if the standard error is added to or subtracted
308 from the mean (Figure 6a, 6b, 6c). The data-collection time, spatial variation and variations of
309 other topographic features can also introduce bias across sites. However, as data-collection time
310 in this study only differed by a few days, *in situ* snow-depth sensor data suggest that the melting
311 and densification effect was under 2 cm (https://czo.ucmerced.edu/dataCatalog_sierra.html). As
312 for other topographic variables, the observation of a slope effect, shown as the trend lines in
313 Figure 7a and the negative regression coefficients of the two linear-regression models, could be
314 explained by steeper slopes having higher avalanche potential, fewer trees and thus more wind;
315 and thus some snow is more likely to be lost from these slopes. Snowpack located in south-
316 facing slopes receives higher solar radiation, with the snowmelt being accelerated (Kirchner et
317 al., 2014). This explains the trends observed in Figure 7b and the negative regression coefficients
318 of the multivariate models. Although Lidar has measurement errors caused by slope and aspect
319 (Baltsavias, 1999; Deems et al., 2013; Hodgson and Bresnahan, 2004), the error is not able to be
320 quantitatively traced back to each variable; and we assumed that its influence on the trends could
321 be neglected. As canopy interception results in reduced snow depth under canopy, the snow-
322 depth residuals are found changing from negative to positive with penetration fraction and the
323 regression coefficients are positive (Figure 7c). The multivariate linear-regression model built

324 from the Lidar data is a significant improvement, as the variability of the snow distribution could
325 explain 15-25% more than the univariate linear-regression model with elevation as the only
326 predictive variable (Table 4) and the estimation bias has a narrower distribution (Figure 10a,
327 10b). Also, fitting an individual linear-regression model for each site is slightly better than using
328 a general model with all data combined (Figure 10c, 10d). This may be because an individual
329 model can capture regional micro-climate within a site better than a general model. The opposite
330 trend of the relative importance of predictive variables observed in Shorthair is because it is a
331 relatively flat site (Figure 1, Figure 8), which implies that topographic variables other than
332 elevation need to be considered when studying areas with small elevation ranges.

333 **4.3 Vegetation effects on snow distribution along elevation**

334 Under-canopy snow distribution is governed by multiple factors that affect the energy
335 environment, as observed by melting (Essery et al., 2008; Gelfan et al., 2004) and accumulation
336 rates (Pomeroy et al., 1998; Schmidt and Gluns, 1991; Teti, 2003). Our results show different
337 responses when comparing the snow-depth difference between open and canopy-covered areas
338 between study sites (Figure 9a). In the rain-snow transition zone from 1500 to 2000 m at
339 Providence we see a sharp linear increase between open and under-canopy snow depth that is
340 likely governed by the under-canopy energy environment and the canopy-interception effect on
341 precipitation, which accelerate snowmelt and prevent accumulation of under-canopy snow.
342 Above 2000 m, the snow-depth difference observed at Bull and Shorthair stabilized around 40
343 cm and 20 cm respectively, with fluctuations less than 10 cm along elevation. Breaking from this
344 pattern, the large dip in snow-depth difference, down to 10 cm, observed at Wolverton at
345 elevations of 2250-2750 m deviates from the 35-40 cm plateau. Also, the snow-depth difference
346 at Shorthair stabilizes around 20 cm, which is 20 cm lower than the stabilized value at Bull.

347 Based on the scatterplots shown in Figures 6a and 6b that are color coded by northness, at an
348 elevation range of 2300-2700 m, there are a lot more data points with both low snow depth and
349 extremely negative northness in the open area than under the canopy, which implies that
350 anisotropic distribution of other topographic variables is affecting the snow-depth difference.
351 This is further shown by filtering out the data points not within a small certain range (-0.1 to 0.1)
352 of northness, and then reproducing Figure 9a using the filtered data. As presented in Figure 11, it
353 is apparent that the large dip at Wolverton is flattened out owing to a canopy effect of around 25-
354 45 cm. Thus a sigmoidal function was used to characterize the snow-depth difference changes
355 with elevation, excluding topographic interactions. The interactions between topographic
356 variables and vegetation is most likely attributable to the under-canopy snowpack being less
357 sensitive to solar radiation versus snowpack in the open area (Courbaud et al., 2003; Dubayah,
358 1994; Essery et al., 2008; Musselman et al., 2008, 2012).

359 In spite of filtering the topographic effect, there is still about a 20-cm magnitude of
360 fluctuation in the snow-depth difference, which might be attributed to various clearing sizes of
361 open area at different locations and various vegetation types in forests (Hedstrom and Pomeroy,
362 1998; Pomeroy et al., 2002; Schmidt and Gluns, 1991); however, we were not able to explore
363 these features of the sites from the current Lidar dataset.

364 **5. Conclusions**

365 The rasterized Lidar data show that the percentage of pixels with at least one ground
366 return, and thus a snow-depth measurement, increases from 65-90% to 99% as the sampling
367 resolution increases from 1 m to 5 m. However, this coarser resolution may mask undersampling
368 of under-canopy snow relative to snow in open areas. With about 28% of the area in dense
369 mixed-conifer forest having no returns, using snow depths in open areas as estimates of snow

370 depth under dense canopies would result in at least a 10-cm overestimation error in the average
371 snow depth in the main snow-producing elevations of 2000-3000 m.

372 Using Lidar data gridded at 1-m resolution, average snow depth within each 1-m
373 elevation band shows a strong correlation with elevation and consistent pattern across all sites.
374 The linear-regression models show that elevation explains 43% of snow-depth variability; and
375 that over 57% of the variability is explained when including all physiographic variables. This
376 indicates that snow distribution in the southern Sierra Nevada is primarily influenced by an
377 orographic-lift effect on precipitation. Snow-depth residuals calculated by de-trending the
378 elevation dependency are correlated with slope, aspect and penetration fraction; and the
379 regression coefficients of these variables in the multivariate linear-regression model show that
380 they are statistically significant in explaining the snow-depth variability, all with p-values
381 smaller than 0.01. Over the elevation range of 1500-3300 m, snow depth decreases 1 cm per 1°
382 slope, and decreases 0.5 cm per 1° aspect in going from north to south. In open areas, snow
383 depth increases 2 cm per 10% increase in penetration fraction, while under canopy the snow
384 depth increases 10 cm per 10% penetration-fraction increase. Although the latter three variables
385 were observed to be less important than elevation, the relative importance of all four variables
386 varies with local elevation range and canopy.

387 The snow-depth difference between open and canopy-covered areas increased in the rain-
388 snow transition elevation range and then stabilized around 25-45 cm at high elevation.
389 Fluctuations in certain elevation ranges are attributed part to interactions from other topographic
390 variables. Evidence of this is found by filtering northness into a narrow band, which results in
391 these fluctuations flattening out.

392 *Acknowledgements.* This material is based on data and processing services provided by the
393 OpenTopography Facility with support from the National Science Foundation under NSF Award
394 Numbers 1226353 and 1225810. Research was supported by the National Science Foundation
395 under NSF Award Numbers 1331939 and 1239521 and UC Water Security and Sustainability
396 Research Initiative funded by the University of California Office of the President (UCOP) (Grant
397 No. 13941). We are grateful to M. Sturm and A. Harpold for their thoughtful comments and
398 reviews of this work. Also thank R.D. Brown, Q. Guo, and N.P. Molotch for their helpful
399 comments and J. Flanagan for providing canopy height model data.

400 **Reference**

- 401 Anderson, H. W., Pacific Southwest Forest and Range Experiment Station (Berkeley, CA),
402 California Department of Water Resources: Managing California's Snow Zone Lands for
403 Water, Pacific Southwest Forest and Range Experiment Station, Forest Services, U.S.
404 Department of Agriculture, 1963.
- 405 Bales, R. C., Molotch, N. P., Painter, T. H., Dettinger, M. D., Rice, R. and Dozier, J.: Mountain
406 hydrology of the western United States, *Water Resour. Res.*, 42, W08432,
407 doi:10.1029/2005WR004387, 2006.
- 408 Bales, R. C., Hopmans, J. W., O'Geen, A. T., Meadows, M., Hartsough, P. C., Kirchner, P.,
409 Hunsaker, C. T. and Beaudette, D.: Soil Moisture Response to Snowmelt and Rainfall in a
410 Sierra Nevada Mixed-Conifer Forest, *Vadose Zo. J.*, 10, 786-799, doi:10.2136/vzj2011.0001,
411 2011.
- 412 Baltsavias, E.: Airborne laser scanning: basic relations and formulas, *ISPRS J. Photogramm.*
413 *Remote Sens.*, 54(2), 199-214, doi: 10.1016/S0924-2716(99)00015-5, 1999.
- 414 Barrett, A. P.: National Operational Hydrologic Remote Sensing Center SNOW Data
415 Assimilation System (SNODAS) Products at NSIDC, National Snow and Ice Data Center,
416 Cooperative Institute for Research in Environmental Sciences, 2003.
- 417 Berris, S. N. and Harr, R. D.: Comparative snow accumulation and melt during rainfall in
418 forested and clear-cut plots in the Western Cascades of Oregon, *Water Resour. Res.*, 23(1),
419 135-142, doi:10.1029/WR023i001p00135, 1987.
- 420 Breiman, L.: Random forest, *Mach. Learn.*, 45(1), 5-32, doi:10.1023/A:1010933404324,
421 2001.
- 422 California Department of Water Resources: California's Flood Future: Recommendations
423 for Managing the State's Flood Risk., 2013.
- 424 Cleveland, W. S.: Robust Locally Weighted Regression and Smoothing Scatterplots, *J. Am.*
425 *Stat. Assoc.*, 74(368), 829-836, doi:10.2307/2286407, 1979.
- 426 Clow, D. W., Nanus, L., Verdin, K. L. and Schmidt, J.: Evaluation of SNODAS snow depth and
427 snow water equivalent estimates for the Colorado Rocky Mountains, USA, *Hydrol. Process.*,
428 26(17), 2583-2591, doi:10.1002/hyp.9385, 2012.
- 429 Colle, B. a.: Sensitivity of Orographic Precipitation to Changing Ambient Conditions and
430 Terrain Geometries: An Idealized Modeling Perspective, *J. Atmos. Sci.*, 61(5), 588-606,
431 doi:10.1175/1520-0469(2004)061<0588:SOOPTC>2.0.CO;2, 2004.
- 432 Courbaud, B., De Coligny, F. and Cordonnier, T.: Simulating radiation distribution in a

433 heterogeneous Norway spruce forest on a slope, *Agric. For. Meteorol.*, 116(1-2), 1–18,
434 doi:10.1016/S0168-1923(02)00254-X, 2003.

435 Deems, J. S. and Painter, T. H.: Lidar measurement of snow depth: accuracy and error
436 sources, *Proc. 2006 Int. Snow Sci. Work. Telluride, Color. USA, Int. Snow Sci. Work.*, 330,
437 330–338, 2006.

438 Deems, J. S., Fassnacht, S. R. and Elder, K. J.: Fractal Distribution of Snow Depth from Lidar
439 Data, *J. Hydrometeorol.*, 7(2), 285–297, 2006.

440 Deems, J. S., Painter, T. H. and Finnegan, D. C.: Lidar measurement of snow depth: a review, *J.*
441 *Glaciol.*, 59(215), 467–479, doi:10.3189/2013JoG12J154, 2013.

442 Dubayah, R. C.: Modeling a solar radiation topoclimatology for the Rio Grande River Basin, *J.*
443 *Veg. Sci.*, 5(5), 627–640, doi:10.2307/3235879, 1994.

444 Erickson, T. a., Williams, M. W. and Winstral, A.: Persistence of topographic controls on the
445 spatial distribution of snow in rugged mountain terrain, Colorado, United States, *Water*
446 *Resour. Res.*, 41(4), 1–17, doi:10.1029/2003WR002973, 2005.

447 Erxleben, J., Elder, K. and Davis, R.: Comparison of spatial interpolation methods for
448 estimating snow distribution in the Colorado Rocky Mountains, *Hydrol. Process.*, 16(18),
449 3627–3649, doi:10.1002/hyp.1239, 2002.

450 Essery, R., Bunting, P., Rowlands, A., Rutter, N., Hardy, J., Melloh, R., Link, T., Marks, D. and
451 Pomeroy, J.: Radiative Transfer Modeling of a Coniferous Canopy Characterized by
452 Airborne Remote Sensing, *J. Hydrometeorol.*, 9(2), 228–241, doi:10.1175/2007JHM870.1,
453 2008.

454 Gelfan, a. N., Pomeroy, J. W. and Kuchment, L. S.: Modeling Forest Cover Influences on Snow
455 Accumulation, Sublimation, and Melt, *J. Hydrometeorol.*, 5(5), 785–803, doi:10.1175/1525-
456 7541(2004)005<0785:MFCIOS>2.0.CO;2, 2004.

457 Golding, D. L. and Swanson, R. H.: Snow distribution patterns in clearings and adjacent
458 forest, *Water Resour. Res.*, 22(13), 1931, doi:10.1029/WR022i013p01931, 1986.

459 Goulden, M. L., Anderson, R. G., Bales, R. C., Kelly, a. E., Meadows, M. and Winston, G. C.:
460 Evapotranspiration along an elevation gradient in California’s Sierra Nevada, *J. Geophys.*
461 *Res. Biogeosciences*, 117(3), 1–13, doi:10.1029/2012JG002027, 2012.

462 Grünewald, T., Stötter, J., Pomeroy, J. W., Dadic, R., Moreno Baños, I., Marturià, J., Spross, M.,
463 Hopkinson, C., Burlando, P. and Lehning, M.: Statistical modelling of the snow depth
464 distribution in open alpine terrain, *Hydrol. Earth Syst. Sci.*, 17(8), 3005–3021,
465 doi:10.5194/hess-17-3005-2013, 2013.

466 Grünewald, T., Bühler, Y. and Lehning, M.: Elevation dependency of mountain snow depth,
467 *Cryosph.*, 8(6), 2381–2394, doi:10.5194/tc-8-2381-2014, 2014.

468 Guan, B., Molotch, N. P., Waliser, D. E., Jepsen, S. M., Painter, T. H. and Dozier, J.: Snow water
469 equivalent in the Sierra Nevada: Blending snow sensor observations with snowmelt model
470 simulations, *Water Resour. Res.*, 49(8), 5029–5046, doi:10.1002/wrcr.20387, 2013.

471 Hedstrom, N. R. and Pomeroy, J. W.: Measurements and modelling of snow interception in
472 the boreal forest, *Hydrol. Process.*, 12(10-11), 1611–1625, doi:10.1002/(SICI)1099-
473 1085(199808/09)12:10/11<1611::AID-HYP684>3.0.CO;2-4, 1998.

474 Hodgson, M. E. and Bresnahan, P.: Accuracy of Airborne Lidar-Derived Elevation : Empirical
475 Assessment and Error Budget, *Photogramm. Eng. Remote Sensing*, 70(3), 331–339, 2004.

476 Hopkinson, C., Sitar, M., Chasmer, L., Gynan, C., Agro, D., Enter, R., Foster, J., Heels, N.,
477 Hoffman, C., Nillson, J. and St Pierre, R.: Mapping the spatial distribution of snowpack depth
478 beneath a variable forest canopy using airborne laser altimetry, *Proc. 58th Annu. East.*
479 *Snow Conf.*, Ottawa, Ontario, Canada, 2001.

480 Hopkinson, C., Sitar, M., Chasmer, L. and Treitz, P.: Mapping snowpack depth beneath forest
481 canopies using airborne lidar., *Photogramm. Eng. Remote Sens.*, 70(3), 323–330, 2004.

482 Howat, I. M. and Tulaczyk, S.: Trends in spring snowpack over a half-century of climate
483 warming in California, USA, *Ann. Glaciol.*, 40, 151–156, doi:10.3189/172756405781813816,
484 2005.

485 Hunsaker, C. T., Whitaker, T. W. and Bales, R. C.: Snowmelt Runoff and Water Yield Along
486 Elevation and Temperature Gradients in California’s Southern Sierra Nevada¹, *JAWRA J.*
487 *Am. Water Resour. Assoc.*, 48(4), 667–678, doi:10.1111/j.1752-1688.2012.00641.x, 2012.

488 J. Revuelto, J. I. Lopez-Moreno, C. Azorin-Molina. and S. M. Vicente-Serrano: Canopy
489 influence on snow depth distribution in a pine stand determined from terrestrial laser data,
490 *Water Resour. Res.*, 51, 3476-3489, doi:10.1002/2014WR016496, 2015.

491 Kirchner, P. B.: Dissertation for the degree of Doctor of Philosophy, University of California,
492 Merced., 2013.

493 Kirchner, P. B., Bales, R. C., Molotch, N. P., Flanagan, J. and Guo, Q.: LiDAR measurement of
494 seasonal snow accumulation along an elevation gradient in the southern Sierra Nevada,
495 California, *Hydrol. Earth Syst. Sci. Discuss.*, 11, 5327–5365, doi:10.5194/hessd-11-5327-
496 2014, 2014.

497 Lehning, M., Grünewald, T. and Schirmer, M.: Mountain snow distribution governed by an
498 altitudinal gradient and terrain roughness, *Geophys. Res. Lett.*, 38(19), 1–5,

499 doi:10.1029/2011GL048927, 2011.

500 Mahat, V. and Tarboton, D. G.: Representation of canopy snow interception, unloading and
501 melt in a parsimonious snowmelt model, *Hydrol. Process.*, 28, 6320-6336,
502 doi:10.1002/hyp.10116, 2013.

503 Marks, K. and Bates, P.: Integration of high-resolution topographic data with floodplain
504 flow models, *Hydrol. Process.*, 14, 2109–2122, doi:10.1002/1099-
505 1085(20000815/30)14:11/12<2109::AID-HYP58>3.0.CO;2-1, 2000.

506 McMillen, R. T.: An eddy correlation technique with extended applicability to non-simple
507 terrain, *Boundary-Layer Meteorol.*, 43(3), 231–245, doi:10.1007/BF00128405, 1988.

508 Molotch, N. P. and Margulis, S. a.: Estimating the distribution of snow water equivalent
509 using remotely sensed snow cover data and a spatially distributed snowmelt model: A
510 multi-resolution, multi-sensor comparison, *Adv. Water Resour.*, 31(11), 1503–1514,
511 doi:10.1016/j.advwatres.2008.07.017, 2008.

512 Molotch, N. P., Colee, M. T., Bales, R. C. and Dozier, J.: Estimating the spatial distribution of
513 snow water equivalent in an alpine basin using binary regression tree models: The impact
514 of digital elevation data and independent variable selection, *Hydrol. Process.*, 19(December
515 2004), 1459–1479, doi:10.1002/hyp.5586, 2005.

516 Musselman, K. N., Molotch, N. P. and Brooks, P. D.: Effects of vegetation on snow
517 accumulation and ablation in a mid-latitude sub-alpine forest, *Hydrol. Process.*, 22(15),
518 2767–2776, doi:10.1002/hyp.7050, 2008.

519 Musselman, K. N., Molotch, N. P., Margulis, S. a., Kirchner, P. B. and Bales, R. C.: Influence of
520 canopy structure and direct beam solar irradiance on snowmelt rates in a mixed conifer
521 forest, *Agric. For. Meteorol.*, 161, 46–56, doi:10.1016/j.agrformet.2012.03.011, 2012.

522 Musselman, K. N., Margulis, S. a. and Molotch, N. P.: Estimation of solar direct beam
523 transmittance of conifer canopies from airborne LiDAR, *Remote Sens. Environ.*, 136, 402–
524 415, doi:10.1016/j.rse.2013.05.021, 2013.

525 Nolan, M., Larsen, C. and Sturm, M.: Mapping snow-depth from manned-aircraft on
526 landscape scales at centimeter resolution using Structure-from-Motion photogrammetry,
527 *Cryosph. Discuss.*, 9, 333–381, doi:10.5194/tcd-9-333-2015, 2015.

528 Pedregosa, F. et al.: Scikit-learn: Machine Learning in Python, *The Journal of Machine*
529 *Learning Research*, 12, 2825–2830, 2011.

530 Pomeroy, J. W., Parviainen, J., Hedstrom, N. and Gray, D. M.: Coupled modelling of forest
531 snow interception and sublimation, *Hydrol. Process.*, 12(15), 2317–2337,

532 doi:10.1002/(SICI)1099-1085(199812)12:15<2317::AID-HYP799>3.0.CO;2-X, 1998.

533 Pomeroy, J. W., Gray, D. M., Hedstrom, N. R. and Janowicz, J. R.: Prediction of seasonal snow
534 accumulation in cold climate forests, *Hydrol. Process.*, 16(18), 3543–3558,
535 doi:10.1002/hyp.1228, 2002.

536 Raupach, M. R.: Vegetation-atmosphere interaction in homogeneous and heterogeneous
537 terrain: some implications of mixed-layer dynamics, *Vegetatio*, 91(1-2), 105–120,
538 doi:10.1007/BF00036051, 1991.

539 Rice, R. and Bales, R. C.: Embedded-sensor network design for snow cover measurements
540 around snow pillow and snow course sites in the Sierra Nevada of California, *Water Resour.*
541 *Res.*, 46(3), 1–13, doi:10.1029/2008WR007318, 2010.

542 Rice, R., Bales, R. C., Painter, T. H. and Dozier, J.: Snow water equivalent along elevation
543 gradients in the Merced and Tuolumne River basins of the Sierra Nevada, *Water Resour.*
544 *Res.*, 47(8), n/a–n/a, doi:10.1029/2010WR009278, 2011.

545 Roe, G. H.: Orographic Precipitation, *Annu. Rev. Earth Planet. Sci.*, 33(1), 645–671,
546 doi:10.1146/annurev.earth.33.092203.122541, 2005.

547 Roe, G. H. and Baker, M. B.: Microphysical and Geometrical Controls on the Pattern of
548 Orographic Precipitation, *J. Atmos. Sci.*, 63(3), 861–880, doi:10.1175/JAS3619.1, 2006.

549 Rosenberg, E. a., Wood, A. W. and Steinemann, A. C.: Statistical applications of physically
550 based hydrologic models to seasonal streamflow forecasts, *Water Resour. Res.*, 47(3),
551 W00H14, doi:10.1029/2010WR010101, 2011.

552 Rotach, M. W. and Zardi, D.: On the boundary-layer structure over highly complex terrain:
553 Key findings from MAP, *Q. J. R. Meteorol. Soc.*, 133, 937–948, doi:10.1002/qj.71, 2007.

554 Schmidt, R. a. and Gluns, D. R.: Snowfall interception on branches of three conifer species,
555 *Can. J. For. Res.*, 21, 1262–1269, doi:10.1139/x91-176, 1991.

556 Smith, R. B. and Barstad, I.: A Linear Theory of Orographic Precipitation, *J. Atmos. Sci.*,
557 61(12), 1377–1391, doi:10.1175/1520-0469(2004)061<1377:ALTOOP>2.0.CO;2, 2004.

558 Sturm, M.: Snow distribution and heat flow in the taiga, *Arctic, Antarct. Alp. Res.*, 24(2),
559 145–152, 1992.

560 Teti, P.: Relations between peak snow accumulation and canopy density, *For. Chron.*, 79(2),
561 307–312, 2003.

562 Wigmosta, M. S., Vail, L. W. and Lettenmaier, D. P.: A distributed hydrology-vegetation
563 model for complex terrain, *Water Resour. Res.*, 30(6), 1665–1680,
564 doi:10.1029/94WR00436, 1994.

565 Table 1. Lidar data collection information

	Bull	Shorthair	Providence	Wolverton
Snow-off flight date	August 15, 2010	August 13, 2010	August 5, 2010	August 13-15, 2010
Snow-on flight date	March 24, 2010	March 23, 2010	March 23, 2010	March 21-22, 2010
Area, km ²	22.3	6.8	18.4	58.9
Mean elevation, m	2264	2651	1850	2840
Elevation range, m	1925-2490	2436-2754	1373-2207	1786-3523
Canopy cover, %	51	43	62	30

566

567 Table 2. Flight parameters and sensor settings

Flight parameters		Equipment settings	
Flight altitude	600 m	Wavelength	1047 nm
Flight speed	65 m s ⁻¹	Beam divergence	0.25 mrad
Swath width	233.26 m	Laser PRF	100 kHz
Swath overlap	50%	Scan frequency	55 Hz
Point density	10.27 m ⁻²	Scan angle	±14°
Cross-track resolution	0.233 m	Scan cutoff	3°
Down-track resolution	0.418 m	Scan offset	0°

568 Table 3. Linear-regression results, averaged snow depth vs. elevation in four sites

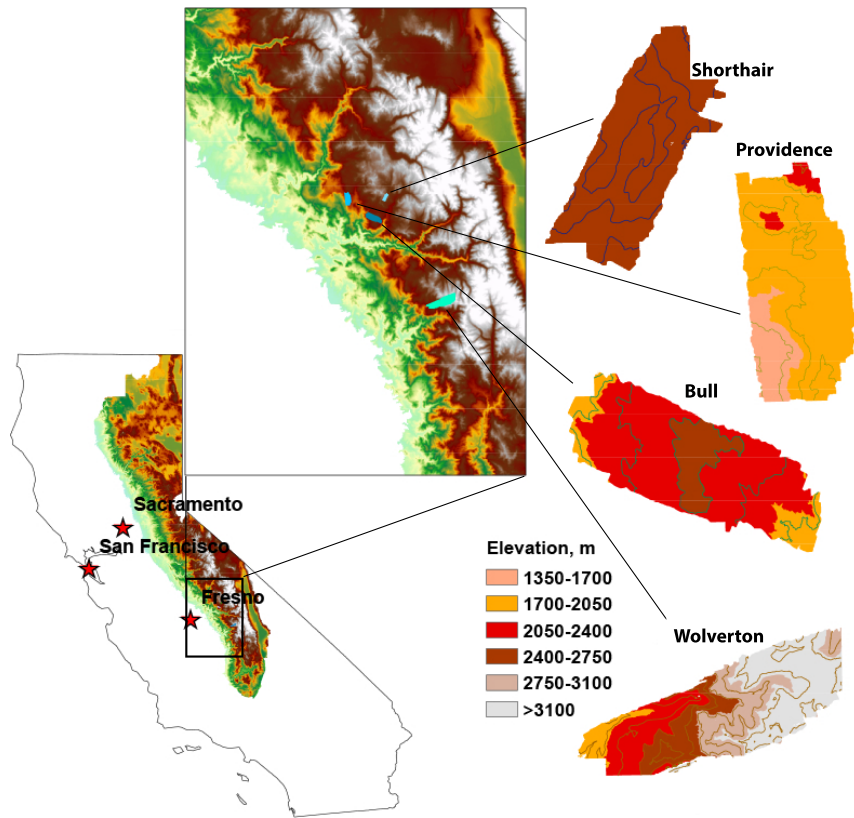
	Bull	Shorthair	Providence	Wolverton
R^2 , open	0.968	0.797	0.931	0.914
R^2 , vegetated	0.978	0.737	0.921	0.972
Slope, open, cm per 100 m	21.6	16.1	37.8	15.3
Slope, vegetated, cm per 100 m	19.9	13.1	26.0	13.4

569

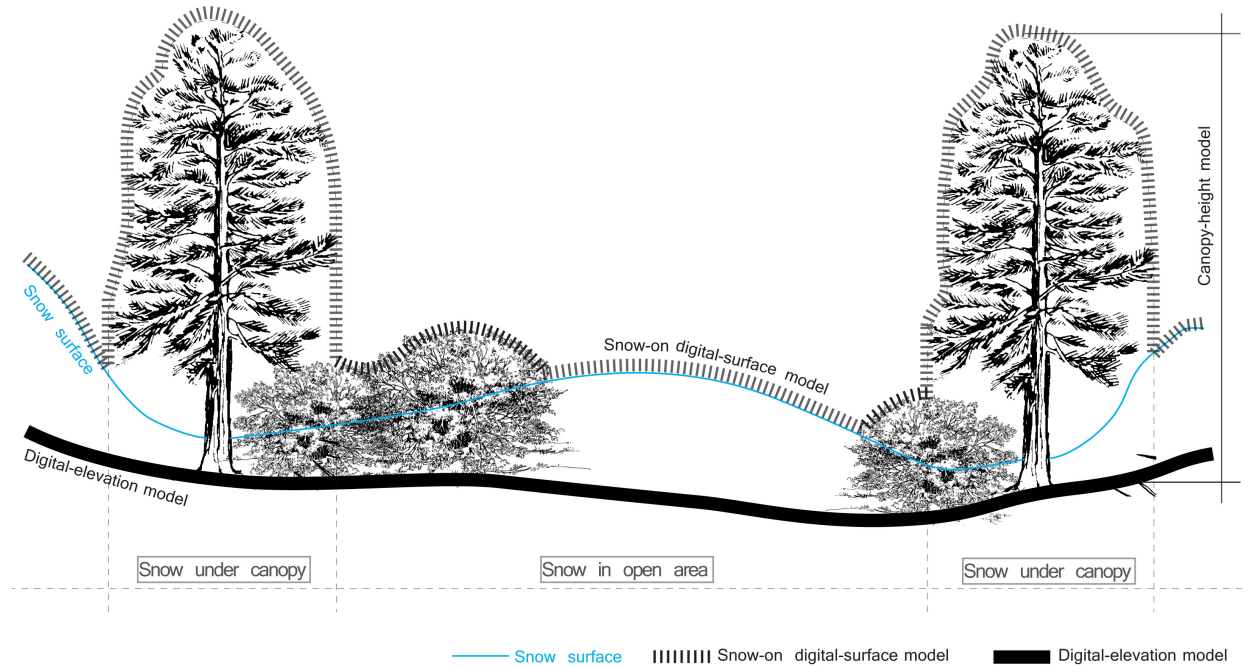
570 Table 4. Coefficients of determination of univariate and multivariate linear-regression models

	Univariate model R ²	Multivariate model R ²
Bull	0.23	0.37
Shorthair	0.06	0.32
Providence	0.39	0.53
Wolverton	0.16	0.38
All sites	0.43	0.57

571

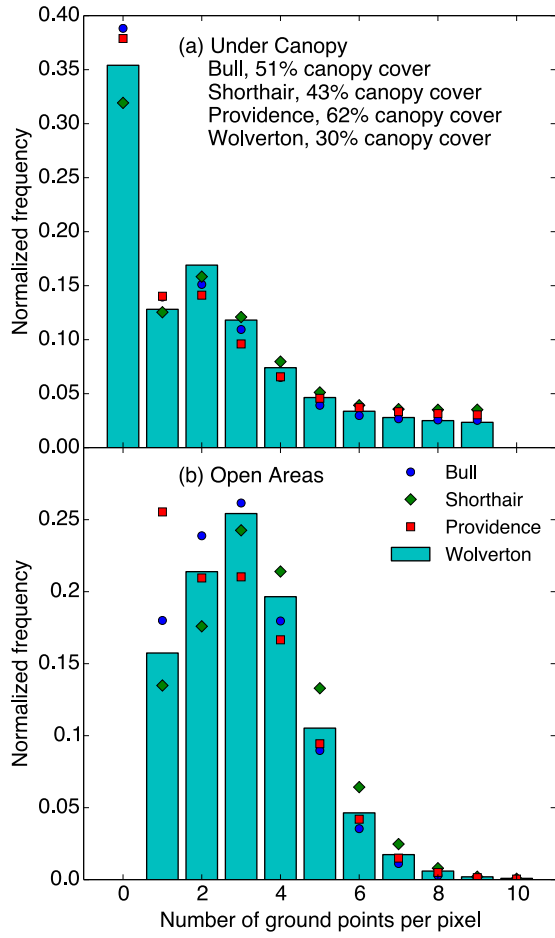


572
 573 Figure 1. Study area and Lidar footprints. (Left) California with Sierra Nevada. (Center) Zoomed view to
 574 show the locations of Lidar footprints. (Right) Elevation and 200-m contour map (100-m for Bull) of
 575 Lidar footprints



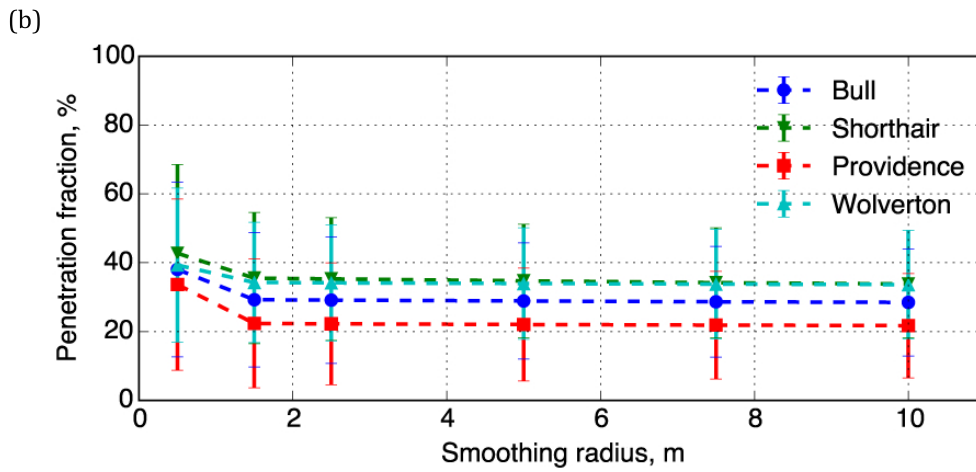
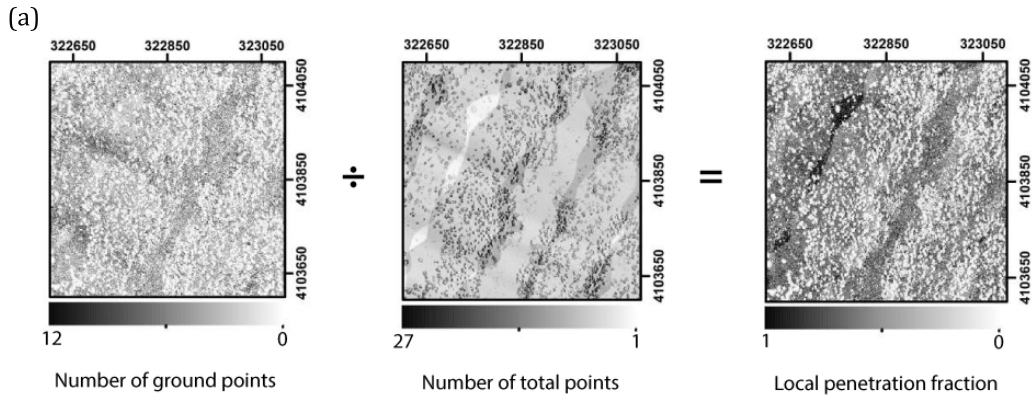
576

577 Figure 2. Subtracting the digital-elevation model from the digital-surface model will result in the canopy-
 578 height model. In this study the height of shrub vegetation is assumed smaller than 2 m while tree
 579 vegetation is taller than 2 m.



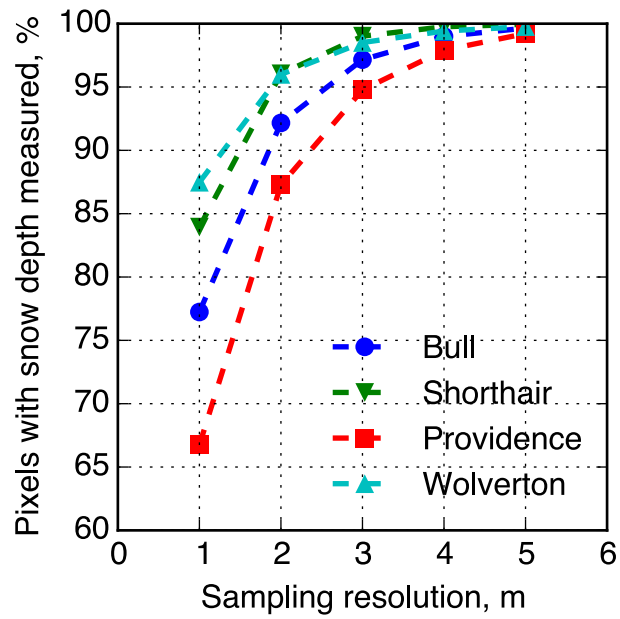
580

581 Figure 3. Normalized histogram of the number of ground points for (a) under-canopy and (b) open 1-m
 582 pixels.



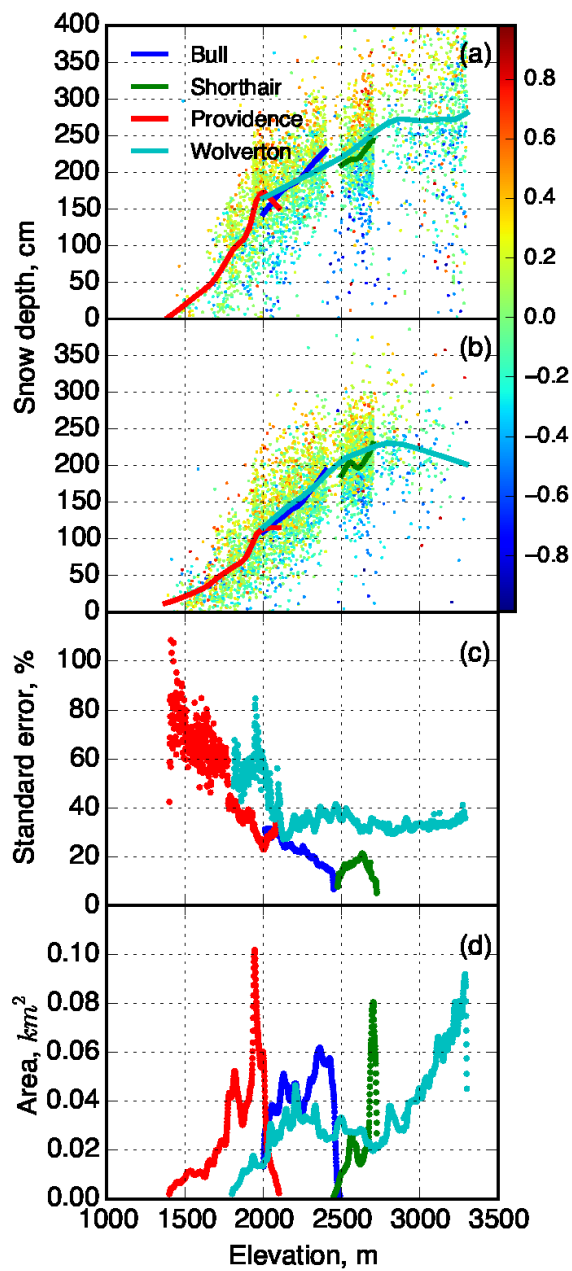
583

584 Figure 4. (a) Dividing the number of ground points of each 1-m pixel by the total number of points in the
 585 pixel gives the penetration fraction of the local pixel. (b) Sensitivity of the smoothed penetration fraction
 586 to the smoothing radius.



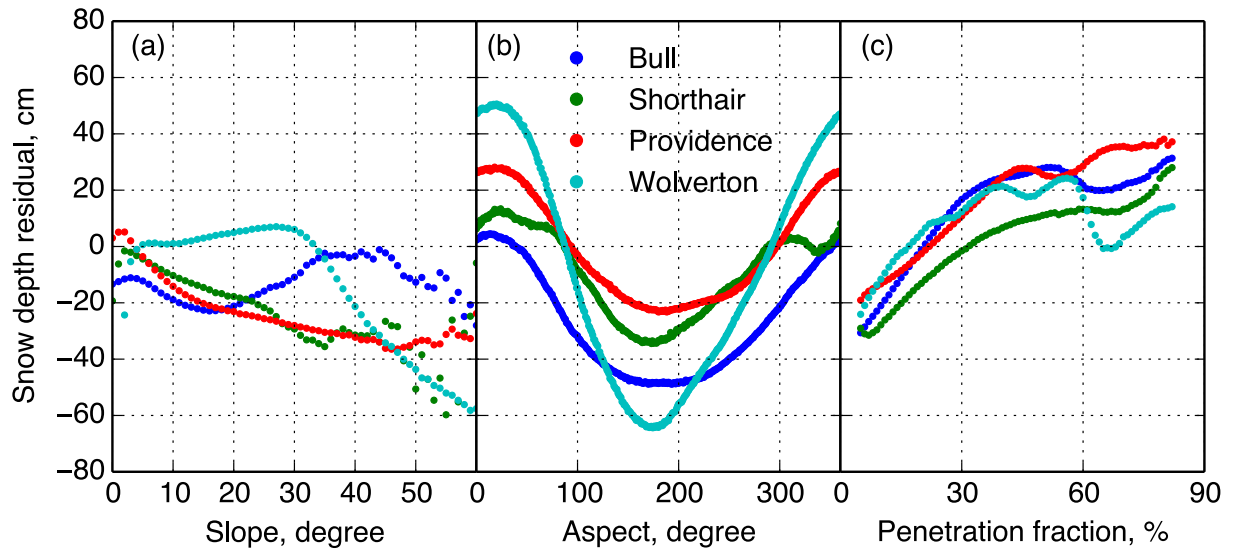
587

588 Figure 5. Sensitivity of the percent of pixels with snow depth measured to the sampling resolution used in
 589 processing the Lidar point cloud at each site.



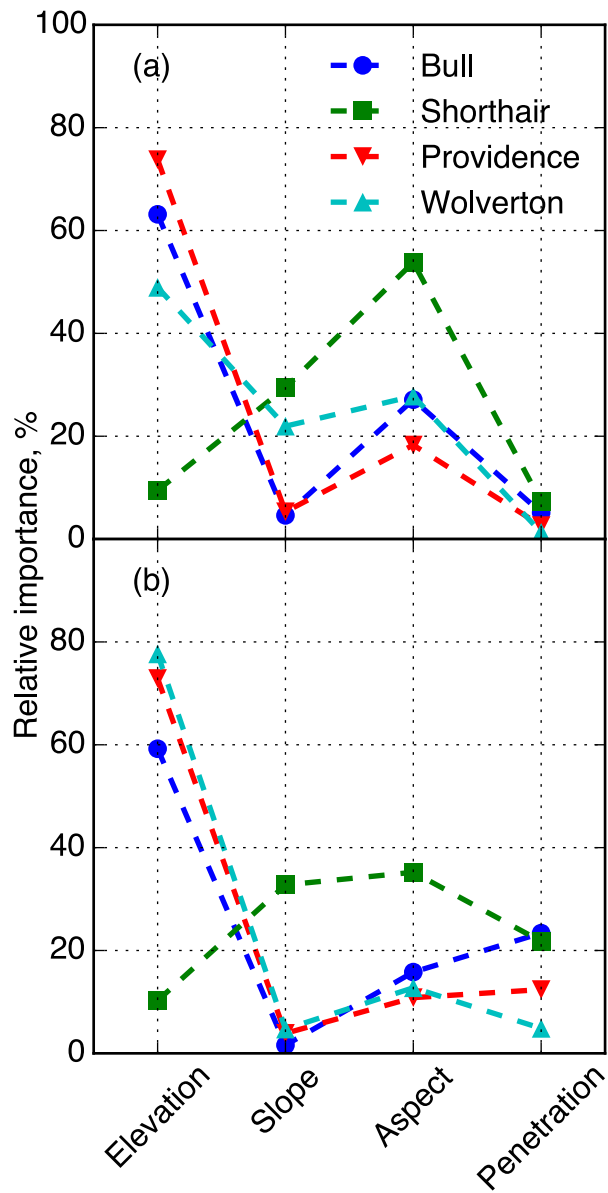
590

591 Figure 6. LOESS smoothed snow depth with northness color coded scatterplot of raw-pixel snow depth
 592 against elevation for (a) open and (b) under-canopy areas. (c) Standard error of the snow depth within
 593 each 1-m elevation band for open area. (d) Total area of each elevation band for both open and under-
 594 canopy areas. Values above 3300 m not shown, where there are few data.



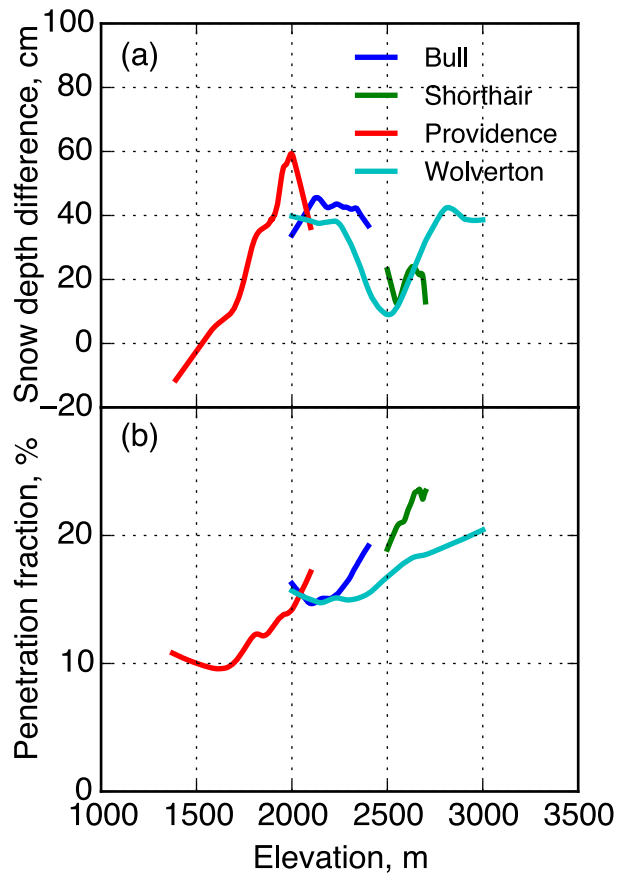
595

596 Figure 7. Average snow-depth residual, calculated as difference between Lidar-measured snow depth and
 597 snow depth from the linear-regression models (open areas) versus: (a) slope, aspect, and (c) penetration
 598 fraction.



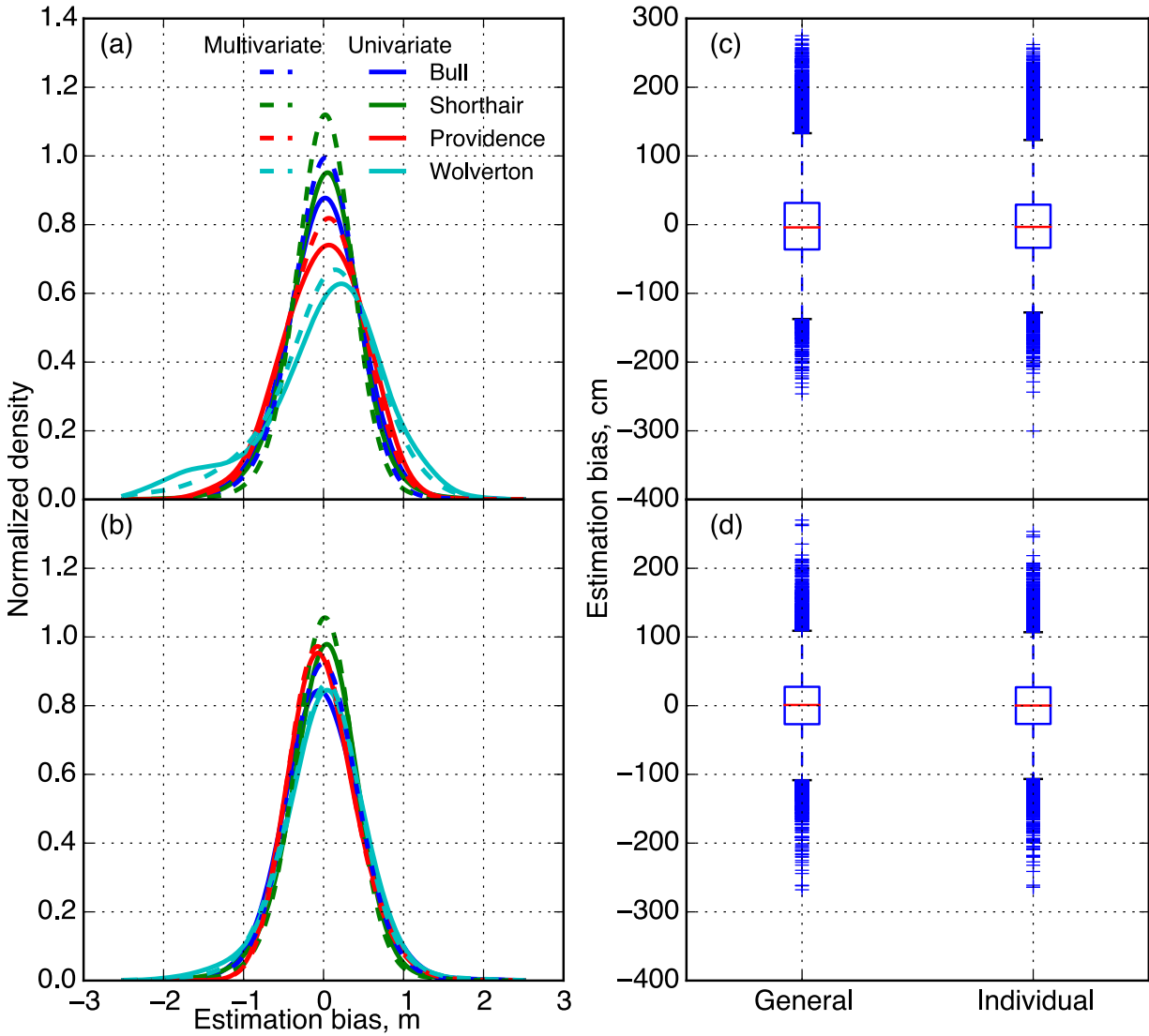
599

600 Figure 8. Relative importance of each physiographic variable in predicting the snow depth from each site
 601 for (a) open area (b) under-canopy area



602

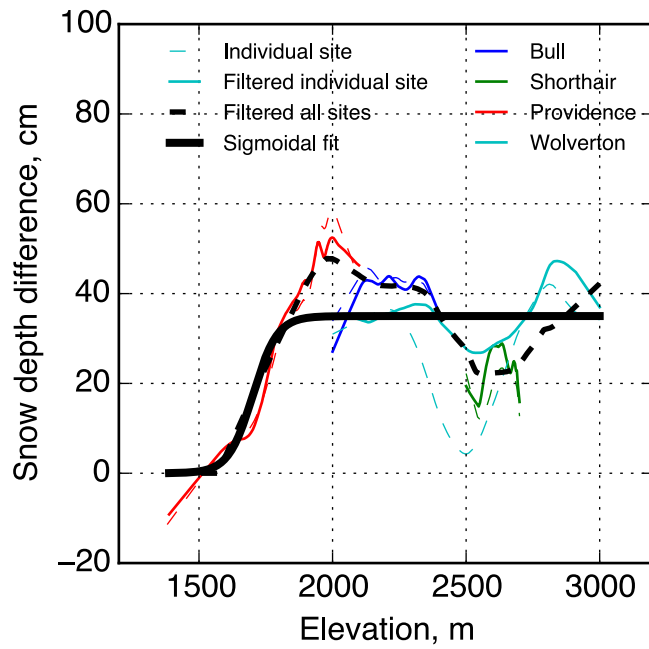
603 Figure 9. (a) Snow-depth difference along elevation for each site calculated from the LOESS smoothed
 604 snow depth. (b) Average penetration fraction versus elevation for each site.



605

606 Figure 10. Normalized density of estimation bias for (a) open (b) under-canopy areas. Estimation bias
 607 boxplots of using one general linear-regression model with all sites' data combined and four linear-
 608 regression models of each individual site for (c) open (d) under-canopy areas.

609



610

611 Figure 11. Snow-depth difference between open and under-canopy areas versus elevation, calculated as
 612 difference between raw 1-m pixel snow depth and northness-filtered 1-m pixel snow depth, together with
 613 the sigmoidal fit of the snow-depth difference.

614